



CHORUS

This is the accepted manuscript made available via CHORUS. The article has been published as:

Space-time correlated two-particle hopping in glassy fluids:
Structural relaxation, irreversibility, decoupling, and
facilitation

Daniel M. Sussman and Kenneth S. Schweizer

Phys. Rev. E **85**, 061504 — Published 25 June 2012

DOI: [10.1103/PhysRevE.85.061504](https://doi.org/10.1103/PhysRevE.85.061504)

**Space-Time Correlated Two-Particle Hopping in Glassy Fluids:
Structural Relaxation, Irreversibility, Decoupling, and Facilitation**

Daniel M. Sussman¹ and Kenneth S. Schweizer^{2,3*}

¹Department of Physics, ²Departments of Materials Science and Chemistry, and ³Frederick Seitz Materials Research Laboratory, University of Illinois, 1304 W. Green Street, Urbana, IL 61801

[*kschweiz@illinois.edu](mailto:kschweiz@illinois.edu)

PACS numbers: 64.70.pv, 61.43.Fs, 64.70.Q-

Abstract

The microscopic nonlinear Langevin equation (NLE) theory of correlated two-particle dynamics in dense fluids of spherical particles is extended to construct a predictive model of multiple correlated hopping and re-caging events of a pair of tagged particles as a function of their initial separation. Modest coarse graining over the liquid structural disorder allows contact to be made with various definitions of irreversible particle motion within the context of a multi-state Markov model. The correlated space-time hopping process that underlies structural relaxation can also be analyzed in the context of kinetically constrained models. The dependence of microscopically-defined mean persistence and exchange times, their distributions, and relaxation-diffusion decoupling on hard-sphere fluid volume fraction is derived from a model in which irreversible jumps serve as the nucleating persistence event. For a subset of questions, the predictions of the two-particle theory are compared with results from the earlier single-particle NLE approach.

I. INTRODUCTION

Understanding at a predictive and microscopic level the slow heterogeneous dynamics in supercooled liquids and colloidal suspensions has been a stubbornly resilient problem in condensed matter science [1–3]. In some ways the field suffers from an embarrassment of riches in the sense that a wide variety of seemingly very different ideas and theoretical methods are able to capture features of glassy dynamics with varying levels of predictive or descriptive power. An incomplete list includes: the random first order transition entropy crisis approach, microscopic force-level theories based on collective density fluctuations (mode coupling theory) and activated particle hopping (nonlinear Langevin equation theory), coarse-grained dynamic facilitation models based on diffusing mobility fields and phenomenological kinetic constraints, potential energy landscape approaches, and the concept of frustration-limited domains [4]. At the same time, issues as fundamental as whether the controlling mechanisms are dynamic, structural, and/or thermodynamic, and whether dynamic heterogeneity is important to first order importance for structural relaxation, remain highly contested [5].

One of the very few approaches that holds the promise of a truly predictive, microscopic, force-level description is mode-coupling theory (MCT) [6,7], which nonlinearly couples liquid relaxation to collective pair-density fluctuations. After invoking approximate projections onto pairs of density modes (or onto coupled density and current modes [7]) and factorizing four-point correlations into products of two-point correlations (a Gaussian-like closure), the collective and self dynamic structure factors can be computed using only the equilibrium pair structure as input. Ideal MCT has had considerable success in the dynamic “precursor” or “crossover” regime in which the relaxation slows down by only a few orders of magnitude. However, the use of a dynamic-closure approximation results in a spurious non-ergodicity transition at a relatively high

temperature in viscous liquids or low volume fraction in particle suspensions. In reality, ergodicity is restored via highly non-Gaussian activated barrier hopping events. Mode-coupling theories that schematically couple to currents have been studied as a way of removing the unphysical non-ergodicity transition [8], but practical formulations that microscopically describe activated hopping events within the traditional ensemble-averaged framework have yet to be constructed. Moreover, even in the precursor regime typically probed in simulation and colloid experiments, very significant dynamic heterogeneities and nongaussian effects are present, all the way down to the single particle level, which are qualitatively missed by ideal MCT [9].

The nonlinear Langevin equation theory of single-particle dynamics [10] is an attempt to address activated hopping microscopically, and has been widely applied to successfully treat diverse colloidal and polymeric systems [e.g., 9, 11, 12]. It is built on a simplified “naïve” version of mode-coupling theory (NMCT) [13] which is qualitatively extended to describe non-Gaussian fluctuations at the stochastic trajectory, not ensemble-averaged, level. The physical motivation for anticipating the usefulness of a self-consistent single-particle approach to describe the alpha relaxation process is the fact that in supercooled fluids single-particle relaxation is strongly coupled to collective pair-density-fluctuation dynamics on the cage scale [14]. For example, simulations find that the mean single-particle alpha relaxation, collective cage relaxation, and shear stress relaxation times are all similar in magnitude and have nearly identical dependences on temperature or density [14, 15]. Similarly, experiments on glassy colloidal suspensions find that self and collective cage dynamic density fluctuation relaxation are closely slaved [16]. In the overdamped colloidal (and model hard-sphere) systems which are the focus of this work, introducing strong and spatially short range attractions changes the pair structure substantially, and the NLE approach is well validated for such repulsive and attractive, spherical

and nonspherical particle systems based on extensive comparison to experiment [11, 17, 18]. The NLE theory does incur significant errors (as do all microscopic approaches) when describing glass-forming viscous liquids, especially in the presence of relatively long range van der Waals attractions [19, 20].

However, for any system the reduction of the glassy dynamics problem to the single-particle level must have limitations. For example, the correlation in space and time of two-particle mobilities directly impacts various dynamic heterogeneity phenomena. We recently extended the single-particle NLE theory to explicitly treat correlated two-particle activated dynamics based on the concept of a dynamic free energy surface, constructed from knowledge of pair structure and which depends on both the thermodynamic state and initial interparticle separation [21]. For hard sphere fluids the theory predicts strong relaxation-diffusion decoupling and stretched exponential relaxation of a specific cage-escape-time correlation function, both of which are in good agreement with experiment and simulation. Moreover, the results provide a resolution to the apparent mystery of how strong decoupling can emerge without a change in the shape of the relaxation time distribution [22, 23]. The hard-sphere two-particle theory also revealed a dynamic correlation length that grows quite modestly from roughly two to three particle diameters over a range of volume fractions in which the relaxation time grew by over three orders of magnitude.

The purpose of the present article is to both extend the two-particle NLE theory to address new questions, and also use the NLE framework to search for connections with other ways of thinking about the glassy dynamics problem. Three topics are addressed. (i) The formulation and application of a multi-state Markov model to describe space-time correlated hopping associated with dynamical interparticle separation (structural relaxation). (ii) A study of

the relative importance of neighbor exchange and neighbor loss in distinguishing irreversible relaxation events from reversible ones [24–26]. (iii) The proposal of a microscopic, structure-based scenario based on modest coarse graining in which the ideas of persistence and exchange that are embedded in phenomenological, kinetically constrained models (KCMs) [27–29] can be identified from the correlated motion of pairs of particles.

Section II briefly reviews the single- and two-particle NLE hopping theories. For economy of expression, we assume the reader has some familiarity with our 2-particle theory [21]. Section III presents new detailed calculations for hard-sphere fluids of dynamic free energy barriers and relaxation times for many initial separations, the key input required to address the three tasks stated above. This information allows the construction of a lightly coarse-grained picture of correlated-in-space-and-time two-particle hopping, in which particles at an initial separation hop to a new relative separation via an activated event, are re-trapped in the spirit of a local equilibrium approximation, hop again after a characteristic time associated with the new relative separation, and so on. In Sec. IV this picture is employed to address the question of irreversible structural relaxation events. The challenge lies in distinguishing between large-amplitude, stochastic fluctuations that ultimately do not relax the system and those that lead to (statistically) irreversible changes to the configuration. In simulations different coarse-graining schemes have been proposed to address this question from the perspective of changes to lists of nearest-neighbor particles [24, 25, 30]. We show that the statistics of such coarse graining schemes can be understood by the statistics of correlated two-particle hops in our NLE theory. Section V makes contact with a different kind of space-time coarse graining that underlies dynamic facilitation models [27–29] and examines its consequences on time-distribution statistics. KCM-like statistics and relaxation-diffusion decoupling can be derived from a

particular coarse-graining over structure in the two-particle hopping picture. We conclude in Sec. VI with a brief summary and outlook. The Appendix suggests an extension of our ideas to improve the venerable Vineyard approximation for the distinct part of the van Hove function.

II. REVIEW OF PRIOR THEORY

Our present work builds on the recent extension of single-particle NLE theory to a two-particle framework that describes transient localization and activated hopping of the center-of-mass (CM) and relative separation of the two particles *as a function of* their initial separation [21]. This section briefly reviews the chief physical ideas; detailed mathematical derivations and discussions of approximations are given in prior papers [10,21,31].

A. Single-Particle Theory

The single (spherical) particle NLE theory is based on a stochastic equation of motion for a tagged sphere, where the scalar displacement of the particle from its initial position, $r(t)$, is the primary dynamical variable of interest. An equation governing its evolution has been heuristically proposed based on three physically-motivated ideas [10, 31]: (i) NMCT correctly predicts localization in the absence of the thermal noise or activated barrier hopping, (ii) particles undergo Fickian diffusion at short times before becoming transiently localized, and (iii) thermal noise destroys the ideal MCT glass transition by allowing for activated hopping. Conditions (ii) and (iii) suggest writing the following nonlinear Langevin equation (in the overdamped regime):

$$-\zeta_s \frac{d}{dt} r(t) - \frac{\partial}{\partial r(t)} F_{dyn}(r(t)) + \delta f(t) = 0, \quad (1)$$

where the white noise δf satisfies the fluctuation-dissipation relation with respect to the short time friction constant ζ_s . The dynamic free energy is constructed so that minimizing it with

respect to displacement recovers the NMCT self-consistency equation for an ensemble-averaged dynamic localization length, $r_{loc} \equiv \langle r^2(t \rightarrow \infty) \rangle \neq \infty$.

NMCT predicts an ideal glass transition within an amorphous Einstein-solid model [13] for the arrested single-particle propagator or Debye-Waller (DW) factor. Invoking a modified Vineyard approximation to relate the single-particle DW factor to its collective analog [31, 32], the NMCT localization equation is

$$\frac{1}{r_{loc}^2} = \frac{1}{9} \int \frac{d\vec{q}}{(2\pi)^3} q^2 \rho C^2(q) S(q) \exp\left(\frac{-q^2 r_{loc}^2}{6} (1 + S^{-1}(q))\right). \quad (2)$$

For hard spheres of diameter σ an ideal glass transition occurs at $\phi_c \equiv \rho_c \pi \sigma^3 / 6 = 0.432$ based on the Percus-Yevick approximation for the direct correlation function and static structure factor, $C(q)$ and $S(q)$, respectively [32]. Combining Eq. (2) with condition (i) above yields an explicit expression for the dynamic free energy:

$$\beta F_{dyn}(r) = -3 \ln(r) - \int \frac{d\vec{q}}{(2\pi)^3} \rho C^2(q) S(q) (1 + S^{-1}(q)) e^{-q^2 r^2 (1 + S^{-1}(q)) / 6}. \quad (3)$$

Its key feature is the emergence of an entropic barrier for volume fractions above ϕ_c . We emphasize that in both the one- and two-particle NLE approaches the relevant aspects of “local structure” that determine the dynamic caging forces, transient localization length, Debye-Waller factors, and intermittent particle trajectories are related to the mean square effective force exerted by the surroundings on the tagged degree(s) of freedom [33]. We also note that the heuristic argument sketched above for arriving at the NLE theory has been buttressed with a non-ensemble-averaged, lightly coarse-grained, dynamic-density–functional-like analysis [31].

B. Two-particle theory

Extending the single-particle NLE theory to treat correlated two-particle motion requires additional physical ideas and approximations [21]. Following the physically-motivated heuristic route, one first constructs an NMCT-like theory for *two* tagged particles based on the assumptions that: (1) momentum relaxes quickly compared to particle displacement, (2) the ensemble-averaged time correlation of forces exerted on the two tagged particles by the surrounding fluid evolves via real (not projected) dynamics, and (3) most importantly, the relevant force-force time correlation functions are not dependent on the instantaneous trajectories of the tagged particles [34]. The last two simplifications imply the central dynamical object is the force-force time correlation function matrix, $K_{\alpha\beta}(t) = \langle \vec{F}_\alpha(0) \cdot \vec{F}_\beta(t) \rangle$, which has a “fast” delta-function component, and a “slow part” associated with structural relaxation.

With the above simplifications the two coupled generalized Langevin Equations governing the center-of-mass (CM) and relative vector coordinates, $\vec{R} = (\vec{r}_1 + \vec{r}_2) / 2$ and $\vec{r} = (\vec{r}_1 - \vec{r}_2) / 2$, are

$$\zeta_0 \frac{d\vec{R}(t)}{dt} = \beta \int_0^t \frac{d\vec{R}(t')}{dt'} K_R(\vec{R}, \vec{r}, t-t') d\tau + \vec{f}^{Q(R)}(t), \quad (4)$$

$$\zeta_0 \frac{d\vec{r}(t)}{dt} = -\frac{1}{\beta} \frac{\partial \ln g(2r+r(0))}{\partial r} + \beta \int_0^t \frac{d\vec{r}(t')}{dt'} K_r(\vec{R}, \vec{r}, t-t') dt' + \vec{f}^{Q(r)}(t). \quad (5)$$

Here $g(r)$ is the radial distribution function, $\vec{f}^{Q(R)}$, $\vec{f}^{Q(r)}$ are random-noise forces, and the superscript Q denotes time evolution according to projected dynamics. The leading term on the right hand side of Eq. (5) represents the “thermodynamic” potential-of-mean-force (PMF) contribution. Here it is written in a fashion that exposes the dependence on initial particle separation, $r(0) \equiv 2|\vec{r}(0)| \equiv r_0$, and implicitly defines the dynamical evolution of the relative

scalar separation coordinate, r . The two equations are coupled via the CM and relative separation memory functions, $K_R(\vec{R}, \vec{r}, t)$ and $K_r(\vec{R}, \vec{r}, t)$, which are approximately obtained in Ref. [21] by standard MCT techniques of projecting the forces onto bilinear products of the center-of-mass or relative coordinate density with the collective fluid density field [32, 35, 36]. A key approximation involves a local-equilibrium idea; our dynamic free energy is not rigorously valid at long times or displacements after an activated event, and so we approximately construct F_{dyn} as a function of initial separation. This naturally leads to an r_0 -dependence of not only the PMF but also explicitly in the memory function K_r . After invoking an additional, physically-motivated approximation involving an angular average (for the isotropic fluid), two coupled NMCT self-consistency relations for the scalar center of mass and relative separation are obtained. These equations can be written in an intuitive equipartition form using the long-time effective spring constants $K_R(t \rightarrow \infty)$ and $K_r(t \rightarrow \infty)$ and the scalar separation coordinates $r^2 = \Delta r^2$ and $R^2 = \Delta \vec{R}^2$ [21]. For very large initial particle separations ($r_0 \gg \sigma$), Eqs. (4) and (5) become equivalent to each other, but owing to the angular-averaging approximation they are very slightly different from the single-particle NLE result [10,21]. Per the single-particle theory, we again interpret these NMCT self-consistency equations as stemming from a force balance, and use them to define a field of effective dynamical forces,

$$\vec{f}(R, r) = f_R(R, r)\hat{R} + f_r(R, r)\hat{r}, \quad (6)$$

where explicit formulas for $f_R \equiv -\partial F_{dyn}(r, R) / \partial R$ and $f_r \equiv -\partial F_{dyn}(r, R) / \partial r$ are given previously [21]. Knowledge of these forces is technically sufficient to construct the NLE evolution equations, which could be numerically solved via stochastic Brownian trajectory simulation [37].

However, by constructing the dynamic free energy surfaces one can both gain much physical intuition and easily compute mean relaxation times using multidimensional Kramers theory.

To determine the dynamical free energy surface, the effective forces must be integrated and added to the PMF, $w(r) = -k_B T \ln g(r)$, to obtain:

$$F_{dyn}(R, r) = \int_C \vec{f}(\vec{l}) \cdot d\vec{l} + (w(2r + r_0) - w(r_0)), \quad (7)$$

where $\vec{l} = R\hat{R} + r\hat{r}$. Since F_{dyn} is not a thermodynamic free energy, the integration is path-dependent. As discussed in detail previously [21], we chose to approximately determine $F_{dyn}(R, r)$ by integrating over the maximally symmetric path: a straight-line diagonal trajectory from the NMCT localization lengths (R_{loc}, r_{loc}) to the point (R, r) .

A representative dynamic free energy surface constructed in this way is shown in Fig. 1. In addition to the two barriers that emerge above the critical volume fraction threshold (nearly parallel to the CM and to the relative coordinate axes), if the initial particle separation is large enough ($r_0 > \sigma$ for hard spheres) then a decrease in the relative separation of the particles is also a permissible motion. Dynamic free energy surfaces can also be constructed corresponding to these motions, except now the change in the PMF must be subtracted, not added, to the path integral over the field of forces:

$$F_{dyn}(R, r^-) = \int_C \vec{f}(\vec{l}) \cdot d\vec{l} - (w(2r + r_0) - w(r_0)). \quad (8)$$

Multidimensional Kramers theory is employed to calculate the mean first barrier-crossing time as function of volume fraction and initial interparticle separation [38]:

$$\frac{\tau}{\tau_0} = \frac{2\pi}{\lambda^+} \left(\frac{|\det \mathbf{K}_B|}{\det \mathbf{K}_0} \right)^{1/2} e^{\beta F_B} \quad (9)$$

Here, $\tau_0 = \beta \zeta_0 \sigma^2$ is the elementary Brownian time scale, F_B is the barrier height, \mathbf{K}_B and \mathbf{K}_0 are the matrices of second derivatives at the saddle point and localization well, respectively, λ^+ is the positive eigenvalue of the matrix $(-\mathbf{D} \cdot \mathbf{K}_B)$, and \mathbf{D} is the matrix of short-time diffusion coefficients in units of the elementary (dilute-limit) diffusion constant D_0 . As in prior work [39], we employ $D_{ij} = \delta_{ij} D_0 / g(\sigma)$, based on Enskog binary collision theory [32]. The prefactor in Eq. (9) varies only weakly with volume fraction and initial separation, and so the mean first-passage time is dominated by the barrier heights. As discussed in detail in [21] the Kramers result is a steepest-descent calculation for the mean first passage hopping time to cross a saddle point in which a pair of particles move from one (metastable) interparticle separation to another, or move together so as to change their CM position, by a displacement of $\sim \sigma / 2$.

III. Multiple Hopping Events and the Role of Initial State

We focus entirely on the *relative* separation of two tagged particles (the r -coordinate), the motion that underlies structural relaxation. This correlated 2-particle displacement can be thought of as an “unbinding” process in which two particles at fixed separation dynamically separate and eventually move independently. The Kramers calculation outline above can be used to separately compute the characteristic time to undergo an activated hopping event in the R , r^+ , and r^- directions. The stochastic dynamics associated with these different processes do not rigorously decouple. If we solved the coupled NLE equations via stochastic trajectory simulation then such dynamical coupling would be naturally included. Here, however, our goals are more

modest and focused solely on exploring a quasi-analytic treatment that only addresses motion directly contributing to *structural relaxation*, i.e. the dynamic randomization of pair correlations embedded in $g(r)$. Since the pair structure is defined by the relative coordinate, we make the simplifying assumption that if an R -barrier hop occurs prior to a hop in the r direction then the r dynamics are unaffected.

In earlier work we reported computations of the dynamic free energy surfaces over a range of volume fractions ($\phi = 0.5 - 0.6$) and at initial separations corresponding to the minima and maxima of the radial distribution function [21]. The primary quantities of interest were the barrier heights and mean first passage times along the direction of CM motion, R , and increasing or decreasing relative separation, r^+ , r^- respectively. In creating a description of “cage escape,” mean first-passage times at many initial separations between the first maximum and first minimum of $g(r)$ were computed. This led to two key predictions: a decoupling between the diffusion constant and the relaxation time (translation-relaxation decoupling) associated with motion in the r -direction of a magnitude and thermodynamic state dependence in semi-quantitative agreement with data on hard sphere suspensions and molecular liquids; and a “cage escape correlation function” that showed stretched-exponential behavior but with a nearly volume-fraction-independent stretching exponent. This qualitative behavior of strong decoupling but no change in the shape of the relaxation function has been observed in hard-sphere simulations [22] and experiments on molecular glass formers [23].

The bulk of the numerical effort in this present work involves the extension of the above program to compute barriers and mean first-passage times at many more values of the initial separation for each volume fraction studied. As detailed in the following sections, this permits

the construction of a more sophisticated description of relaxation events, which in turn allows us to make contact with different ways of looking at the glassy dynamics problem.

Figure 2 presents calculations of the entropic barrier height for motion in the r^+ and r^- directions as a function of initial separation out to the second minima of the radial distribution function. Figure 3 shows the corresponding mean first-passage times. Several points are evident. First, the logarithm of the mean first-passage time closely tracks the barrier height. Second, the barrier heights qualitatively track the PMF at different separations, a fact shown explicitly in Ref. [21]. Third, the mean relaxation time calculations are noisier than the barrier height calculations since small numerical inaccuracies in F_{dyn} are amplified in the calculation of the curvatures required in Eq. (9). This is a second-order effect which does not affect the oscillation of barrier heights/relaxation times on the scale of $g(r)$, a key feature of our analysis. In Fig. 3, spline interpolations are shown which are utilized to smooth the discrete numerical hopping-time data; all our subsequent results are only very weakly sensitive to the specific curve-fitting procedure employed.

In the following sections we adopt a specific jargon and notation to indicate the different types of changes in the relative separation coordinate of two tagged particles. The “hopping” motion of this relative coordinate is often described in the language of a particle hopping, but in reality this means one of the particles is used to define the origin of an instantaneous radial distribution function in the local-equilibrium approximation centered at that particle. Increases and decreases in the relative separation are referred to as forward and backwards hops, respectively, and (consistent with the above notation) superscripts pluses and minuses are employed on both the coordinate itself and the characteristic time to move in a specific direction

$(r^+, \tau^+, r^-, \tau^-)$. Finally, when coarse-graining over shells of the radial distribution function, the characteristic time for the relative coordinate to indicate a change from shell i to shell j is denoted by $\tau_{i \rightarrow j}$.

IV. IRREVERSIBLE NEIGHBOR LOSS AND STRUCTURAL RELAXATION

A. Neighbor Loss, Recovery, and Irreversibility

The notion of “irreversibility” in single-particle statistics of glassy systems has long been a thorny problem. At issue is that a tagged particle spends the majority of its time rattling around in its cage, and then occasionally makes a jump of broadly distributed amplitude, including large displacements of order a particle radius, $\sim \sigma / 2$ [25, 40]. However, such “cage-breaking” jumps do not always lead to an irreversible change in the configuration of the liquid: when viewing trajectories, sometimes the particle hops further away and the cage closes behind it, but other times the particle fluctuates back into the cage, essentially restoring the initial configuration [14,25]. One technique employed in simulations and confocal microscopy experiments on colloids for distinguishing reversible from irreversible rearrangements is to track fluctuations that induce changes in the list of nearest-neighbor particles before and after a tagged particle hops [24, 26, 41].

Our present goal is to address the irreversibility question in the context of the space-time-correlated two-particle hopping model. The physical picture of a particle first hopping some distance and then hopping either further away from or closer to its initial position relative to other particles maps quite intuitively to the combination of our two-particle theory and a local equilibrium idea. The latter means that after a hop the two particles are re-caged and must escape

via another activated event. Our ideas are general with regards to the interparticle pair potential, but we analyze the problem in the context of a hard-sphere fluid.

The relative statistics of a given jump being reversible or irreversible will be treated based on a multi-state Markov model. Additionally, we connect our results to the above-mentioned ideas of nearest-neighbor loss. In particular, we initially determine the probability to first lose some fixed number of neighbors as a function of time, and then study the probability distributions that at time t at least $(x-n)$ nearest neighbors have been irreversibly lost if at some earlier time, $t' < t$, x nearest neighbors were lost. Our results are qualitatively compared to the simulations on model thermal 2D glass formers below the onset temperature [24]. Of course, quantitative comparison between our calculations for a 3D hard sphere fluid and the 2D Lennard-Jones thermal mixture simulations is not possible.

B. Multi-state Markov Hopping Model

The basic spirit of our model is illustrated in the schematic cartoons of Fig. 4. We have previously observed that at all separations a hop in the relative separation coordinate corresponds to a change in r on the order of $\sigma/2$, a natural length scale for defining solvation shells and interstitial configurations [21]. For example, two particles initially at contact can undergo a relative hop that places their separation in an “interstitial”-like configuration, or vice-versa. We use this as motivation to coarse grain over the shells of the radial distribution function, arguing that a forward or backward hop amounts to changing the relative shell the two particles occupy. In this way we track the two-particle separation, computing characteristic times and rates to hop from one shell to the next under the local equilibrium assumption that after a hop the particles temporarily equilibrate and behave as if their new separation serves as the “initial” separation (r_0) of a subsequent hopping event. Since the dynamic free energy surface depends on r_0 via

both the PMF and the dynamical forces of the surrounding particles, subsequent forward and backward hopping events are modified relative to the initial activated motion.

As a more general comment, our focus on large amplitude single and two-particle hopping events should not be interpreted as denying there is more cooperativity involved in the elementary alpha relaxation process. Indeed, the latter no doubt involves the correlated motion, on relatively small scales, of many particles; no microscopic theory exists for such many-particle cooperative dynamics. However, the achievement of irreversibility and structural renewal as defined via neighbor exchange must involve some small number of particles moving a significant fraction of their diameter. It is this latter aspect that we focus on using the NLE approach and our present lightly coarse-grained description. In this regard, we note there is simulation and experimental evidence that on the alpha relaxation time scale the key motions involve compact clusters of particles (not the strings relevant at earlier times) [42, 43]. Moreover, irreversible structural rearrangements have been experimentally imaged in glassy hard-sphere colloidal systems, where compact rearranging regions always involve a few particles displacing by distances of order their radius, dressed by small correlated motions of surrounding colloids [41]. The relationship between the smaller and large displacements, and whether “one triggers the other,” remains poorly understood.

Previously we evaluated the time for two particles initially at contact (i.e., within the first shell of the radial distribution function, $\sigma \leq r_0 \leq g_{min}$, where g_{min} is the first minima of $g(r)$) to first separate, defining a “cage escape” time, $\tau_{cage} = \tau_{1 \rightarrow 2}$, analogous to an alpha-relaxation time [21]. We assumed that the white-noise-driven hopping over a (high) barrier is a Poissonian

process [37], so that the probability to hop from an initial separation r_0 at time t in either the forward or backwards direction is given by

$$P(t, \tau^\pm(r_0)) = \frac{t}{(\tau^\pm(r_0))^2} e^{-t/\tau^\pm(r_0)}. \quad (10)$$

Then, averaging over *both* the dynamic disorder of this Poisson process, and the static disorder from coarse-graining $g(r)$, the probability to exit the cage of nearest neighbors is

$$\tau_{1 \rightarrow 2} = \frac{\int_1^{g_{min}} r_0^2 g(r_0) \int_0^\infty t P(t, \tau^+(r_0)) dt dr_0}{\int_1^{g_{min}} r_0^2 g(r_0) dr_0}. \quad (11)$$

Similarly, the average hopping time from site 2 to 3 is

$$\tau_{2 \rightarrow 3} = \frac{\int_{g_{min}}^{g_2} r_0^2 g(r_0) \int_0^\infty t P(t, \tau^+(r_0)) dt dr_0}{\int_{g_{min}}^{g_2} r_0^2 g(r_0) dr_0}, \quad (12)$$

where g_2 is the location of the second peak of $g(r)$. The other rates are computed analogously, using either the forward or backwards hopping times in $P(t, \tau(r_0))$ as appropriate.

Treating the question of irreversibility requires the determination of how often a particle is recovered after it first jumps away. To do so, we separately consider the probability of first leaving the contact shell, and then the probability of returning given that the particle has left. The first of these questions is straightforward. Defining the function

$$P'(t, \tau^\pm(r_0)) = \int_0^t P(t', \tau^\pm(r_0)) dt' = 1 - e^{-t/\tau^\pm(r_0)} \left(1 + \frac{t}{\tau^\pm(r_0)} \right), \quad (13)$$

as the probability for two particles separated by r_0 to have a jump in their relative separation by time t , and averaging over the spatial disorder in the first shell, gives the probability that by time t a particle has escaped from the first (contact) shell:

$$p(t) = \frac{\int_1^{g_{min}} r_0^2 g(r_0) P'(t, \tau^+(r_0)) dr_0}{\int_1^{g_{min}} r_0^2 g(r_0) dr_0}. \quad (14)$$

To determine whether this escape is irreversible or not we construct a simple 4-site Markov model as schematically illustrated in Fig. 4B, with each site corresponding to a shell of the radial distribution function. Particle separations can hop back and forth between three sites corresponding to the two particles being nearest neighbors, next-nearest neighbors, and next-next-nearest neighbors. The fourth shell of $g(r)$ is treated as a semi-absorbing boundary, in that particles can continue to hop further away but cannot hop back to the third shell (schematically shown in Fig. 4B and represented in the transfer matrix in Eq. (15) below). Over the time scales that we study this (easily relaxed) approximation makes no quantitative difference to our results. Average hopping rates between these shells are computed in complete analogy with the above, taking the mean rates to be the inverse of the mean hopping times. Concretely the model assumes that if the particles hop “forward” from the third site then they never return to being nearest-neighbors. That is, particles can hop back and forth between contact and the second shell, but once they are separated by more than this distance they are never recovered. Rigorously this will not always be true, but on the time scales we consider, and those examined in the simulations (on the order of the mean alpha time, i.e. to hop from the first to the second site), the exceedingly low probability of a recovery makes this a reasonable approximation. We could, of course, use a more sophisticated semi-Markov model that takes into account the Poisson hopping processes instead of using such processes to define the rate constants, but we expect such an improvement to make only a modest quantitative change to our ultimate predictions.

The 4-site Markov model can be easily solved to give the probability, $p_c(t)$, that the particles occupy the “nearest-neighbor” site at time t . We define a transition matrix as

$$T = \begin{pmatrix} -\tau_{1 \rightarrow 2}^{-1} & \tau_{2 \rightarrow 1}^{-1} & 0 & 0 \\ \tau_{1 \rightarrow 2}^{-1} & -(\tau_{2 \rightarrow 3}^{-1} + \tau_{2 \rightarrow 1}^{-1}) & \tau_{3 \rightarrow 2}^{-1} & 0 \\ 0 & \tau_{2 \rightarrow 3}^{-1} & -(\tau_{3 \rightarrow 4}^{-1} + \tau_{3 \rightarrow 2}^{-1}) & 0 \\ 0 & 0 & \tau_{3 \rightarrow 4}^{-1} & -\tau_{4 \rightarrow 5}^{-1} \end{pmatrix} \quad (15)$$

and numerically solve for its eigenvalues λ_i and eigenvectors ξ_i . The initial condition is

$\sum_{i=1}^4 a_i \xi_i = \{1, 0, 0, 0\}$, i.e. the two tagged particles are initially nearest neighbors. The probability of

occupying the nearest-neighbor site is then just the first element of $\sum_{i=1}^4 a_i \xi_i e^{\lambda_i t}$. Combining this

result with Eq. (14) which gives the probability that the particles have ever left contact, $p(t)$, the probability to regain a nearest-neighbor contact given that such a contact was lost (i.e. the probability that a particle was “recovered”) is estimated as

$$p_r(t) = \frac{p_c(t) - (1 - p(t))}{p(t)}. \quad (16)$$

Addressing the irreversibility question at the characteristic time to first hop away, the probability of a typical jump being irreversible is $1 - p_r(\tau_{1 \rightarrow 2})$; this quantity is plotted in the inset of Fig. 5A. We emphasize that a large hop ($> \sigma/2$) is *not* necessary for a jump to be irreversible; even a jump to the interstitial site has a chance to be deemed irreversible with our definition, as we demonstrate in the numerical calculations presented below. The non-monotonicity observed is a highly non-trivial prediction that results from the complex interplay between forward and backwards hopping times, both of which grow with volume fraction but do so at different rates. We note that such a weak non-monotonicity, and an irreversible-jump-

fraction magnitude close to our calculation, has been observed in binary Lennard-Jones mixture simulations as a function of inverse temperature [25]. Our interpretation for irreversibility is then that a particle trying to escape its cage of neighbors must first hop into an “interstitial” site corresponding to the first minimum of the radial distribution function. From there, the average structural constraints determine the relative rates of continuing the cage escape process (“unbinding”) or falling back (“recovery”) into the nearest-neighbor position.

If one assumes that the different particles forming the cage leave and return in an uncorrelated manner, a simple binomial model suffices for the probability that n lost neighbors were recovered given that x nearest neighbors were at some point lost:

$$P_{n,x}(t) = \binom{x}{n} p_r(t)^n (1 - p(t))^{x-n}. \quad (17)$$

The idea that the neighbors can be treated in this uncorrelated manner is perhaps reminiscent of the finding that local density does not correlate well with local dynamic propensity in a constrained lattice gas simulation [44]. Indeed, the distribution of nearest and next-nearest neighbor vacancies found in the simulation is qualitatively quite similar to our $P_{n,x}$ distributions.

Figure 5A shows calculations for various x at $t = \tau_{1 \rightarrow 2}$ and $\phi = 0.55$; qualitatively the results are very similar to the distributions observed in 2D simulations of a binary LJ mixture model below the onset temperature [24]. Figure 5B presents calculations at just two different values of neighbors initially lost but for different volume fractions, and the observed volume fraction dependence of $P_{n,x}$ is rather weak. One can then *define*, as was done in analyzing the simulation data, an event to be irreversible as the value of x such that probability of recovering all of the lost particles falls below some threshold at the characteristic relaxation time,

e.g., $P_{0,x}(\tau_{cage}) < 0.05$. In two dimensions at one specific temperature Widmer-Cooper et al. found $x = 4$ [24], and an experimental study of 2D slices of an ultra-dense 3D hard-sphere colloidal suspension reported $x = 3$ [26]. We estimate that for hard-spheres in three dimensions one also expects $x = 4$ over a broad range of volume fractions, except at the lowest and highest volume fractions we study ($\phi = 0.5 - 0.53, 0.59, 0.60$) where a greater fraction of jumps fail to return to contact and the critical x drops to 3. We also find that this distribution often peaks at $n = x - 2$, as has been reported in the 2D simulation, but we expect this is a coincidence and not a general result. Note that a slightly different definition of “recovery” was used in the simulations: a neighbor was counted as “recovered” at time t if it has been recovered *at any time* prior to t , even if it was then subsequently lost and no longer in the neighbor list at t .

We can also compute quantities like the probability distribution to *first* lose a fixed number of neighbors, a property that has been studied via the 2D simulations [24]. Results for the probability to first lose the fourth neighbor are presented in Fig. 6; the inset shows this quantity up to $t / \tau_{cage} = 2 / 7$, roughly the range studied in the simulations and over which the probability is a monotonically increasing function. We predict that, for the two volume fractions examined, the distribution peaks soon thereafter, and then quickly decays to zero.

V. FACILITATION, KCM STATISTICS, AND DECOUPLING

A. KCM Picture

In this section we propose a specific spatial coarse-graining over activated two-particle motion to try to connect our microscopic theory that relates structure and slow intermittent activated dynamics with the ideas of dynamic facilitation that form the cornerstone of kinetically

constrained models. The KCMs seek to phenomenologically provide a coarse-grained description of glass-formers in the language of lattice spin models. Rules governing the spin flips are chosen so that all configurations are equally likely – resulting in trivial thermodynamics – but where at low temperatures relaxation is governed by increasingly rare diffusing defects, leading to non-trivial dynamically facilitated behavior. Although the microscopic origin of the dynamic rules at the level of atoms and forces is unclear, specific KCMs have been shown to be capable of describing some statistics that result from coarse-graining atomistic MD simulations, and can describe many features of dynamic heterogeneity [29, 45, 46]. In our opinion, there must be some structural basis for the postulated kinetic rules, and searching for them is our present goal. While a first-principles coarse graining of particle trajectories to recover the facilitation rules of specific KCMs (e.g. the Fredrickson-Andersen or East model) does not seem to be a feasible task, one can ask if the statistics of coarse grained particle mobility are similar to the KCM predictions. Here we take a modest first step towards connecting with KCMs, and do not address the full, most-recently proposed picture [29].

Fundamental to the KCM perspective of diffusion-relaxation decoupling is the division of events into “persistence” and “exchange,” which correspond to the first nucleation of particle mobility and subsequent manifestations of mobility, respectively. The basic insight behind this division is the idea that once particle mobility has been nucleated at a site, further mobility becomes more likely at that site. In the facilitation picture, a particle spends a long time waiting for a (rare) excitation line to sweep past, but once an excitation line is in the particle’s vicinity it is very likely it will diffuse back and forth across the particle’s position, triggering further relaxation and diffusion. It is first and foremost this division that we seek to understand at a microscopic level in the present paper.

B. Dynamical Mapping and Model Calculations

Current attempts to coarse-grain particle trajectories from molecular dynamics (MD) simulations onto KCM statistics have relied on interpreting the distribution of persistence and exchange times as the first time a particle moves beyond a threshold distance and then subsequent times between further, similarly-large particle motions. This characteristic threshold is often taken to be half a particle diameter, $a = \sigma / 2$ [45], quite similar to our earlier study of particle escapes from a nearest-neighbor list [21]. Qualitatively similar features are found for a range of choices for this threshold displacement provided that irrelevant small-amplitude vibrational motions are coarse grained out (either by averaging over short vibrational periods or by resolving only inherent structures) and that the displacement is not so large as to obscure a longer time scale associated with broader system relaxation [29].

We adopt the above perspective as inspiration for the analysis of our real-space NLE theory of correlated two-particle hopping. However, we emphasize that the distinction between “persistence” and “exchange” in our microscopic theory arises from the underlying structure of the fluid; spatial correlations imprinted on the hopping times as a function of r_0 make some interparticle separations more favorable for activated events to occur than others. We will take the fundamental persistence event to be the *irreversible* separation of two particles from the first to the second shell of the radial distribution function (Fig. 4B). This definition is in the spirit of recent work on KCMs, where excitations are viewed as “non-trivial particle displacements associated with transitions between relatively long-lived configurations” [29]. That is, since excitations are not just particles moving but an underlying feature of the structure that promotes mobility, we wish to exclude from our definition of “persistence” events those particles motions

which quickly lead to a return to the original configuration. Using the notation of section IV, the probability distribution of a persistence event at a fixed initial separation can thus be described as

$$P_{persist}(t, \tau^+(r_0), \tau^-) = \int_0^t P(t', \tau^+(r_0)) (1 - P'(t-t', \tau^-)) dt', \quad (18)$$

where $P(t, \tau^+(r_0))$ (given by Eq. (10)) is the probability to separate from contact at time t given a mean first-passage time of such an event $\tau^+(r_0)$, and $(1 - P'(t-t', \tau^-))$ from Eq. (13) is the probability that the particle pair has not returned to contact in the time interval $(t-t')$ given a mean time for such an event τ^- . As in our previous work [21], this distribution is then averaged over the spatial disorder in the first shell, taking for convenience the backwards-hopping, irreversibility-revoking events to occur at the characteristic rate $\tau_{2 \rightarrow 1}$ as computed in the previous section. Thus, our final estimate for the persistence time distribution is

$$P(\tau_p) = A \int_1^{g_{min}} r_0^2 g(r_0) P_{persist}(\tau_p, \tau^+(r_0), \tau_{2 \rightarrow 1}) dr_0, \quad (19)$$

with A the normalization constant.

The distribution of Eq. (19) is plotted in Fig. 7 for a variety of hard-sphere-fluid volume fractions, and its first moment is plotted versus volume fraction in Fig. 9. We note that the variance of this distribution closely tracks the mean, a feature of many distributions in the exponential family. A key feature of the best-supported facilitated models is a parabolic-law dependence of the relaxation time [47], and this is clearly shown by the fitting curve in Fig. 9. Specifically, over the range $\phi = 0.5 - 0.6$ the calculations are very well described by $\ln(\tau_p / \tau_0) \propto (\phi - \phi_c)^2$ for volume fractions greater than an empirical onset $\phi_c \approx 0.47$. This is greater than the NMCT crossover volume fraction of $\phi_{NMCT} \approx 0.43$, and in the single-particle theory corresponds to a small barrier of $F_b \approx 0.6 k_B T$.

Consistent with the above we then define the exchange-time distribution as arising from forward hops out of the second shell (i.e. the probability of hopping away before hopping back to contact), which up to a normalization constant B results in

$$P(\tau_x) = B \int_{g_{min}}^{g_{max}^{nd}} r_0^2 g(r_0) P(\tau_x, \tau^+(r_0)) (1 - P'(\tau_x, \tau^-(r_0))) dr_0. \quad (20)$$

Numerical results for this distribution are also plotted in Fig. 7. We note that the decision to exclude backward hops in the definition of an exchange event makes only a very minor quantitative difference to the distribution, but choosing these *irreversible* hops to be the fundamental persistence event in Eq. (19) is important. This choice results in a small quantitative adjustment to the mean persistence time, but qualitatively suppresses much of the short-time part of the distribution since backward hops can occur more rapidly than the cage-breaking event, and emphasizes the large skew of the distribution, consistent with observed persistence distributions in the literature [45, 46, 48].

Figure 8 plots both distributions, normalized by their peak height and position. One sees that the persistence and exchange distributions are significantly different in both their shape and response to increasing volume fraction. Thus, it appears we recover this fundamental feature of KCMs, but do note that some details of our distributions are unlike those deduced in the coarse-grained atomistic MD simulations [45]. In particular, in that work the exchange-time distribution acquires a (slight) skewness opposite that of the persistence-time distribution, whereas we find a slight skewness of the same sign. Additionally, at the lowest two temperatures studied in the MD simulations the peak of the exchange distribution showed almost no shift, whereas we find the peak monotonically shifts to longer times with increasing volume fraction.

The short-time behavior of the exchange-time distributions exhibit the expected Poissonian behavior, but the rest of the exchange-time distribution is a less-good match to observed distributions in simulations of the thermal liquid model. We expect this is partly a result of including only *one* type of exchange event: hopping from the second shell to the third. In reality, one should likely include the statistics of all other types of hops in the exchange time distribution: hopping back and forth from the third shell, center-of-mass hops that we have neglected here, and so on. Additionally, particularly for the relatively low barrier hops that characterize the exchange events, it is known that our choice of a Poissonian distribution for the barrier-hopping process is quantitatively inaccurate [49]. All of these factors would serve to broaden our predicted exchange time distribution in line with what is observed computationally, where particles are typically tracked over relatively long time scales thereby allowing for the sampling of long exchange times [45].

Within the KCM perspective the difference between persistence and exchange times has been proposed to explain the Stokes-Einstein decoupling of viscosity (or alpha relaxation time) and diffusion observed in supercooled liquids and also models of hard sphere suspensions [45, 46, 48]. The argument is that while relaxation is governed by the slowest (most local) characteristic time scale of the system, τ_p , mass transport requires multiple hops to become diffusive and is controlled by the faster exchange processes, and hence proceeds on the time scale τ_x . Thus, the ratio $R = \tau_p / \tau_x$ provides a quantitative measure of the decoupling in a given model. For the hard-sphere system, our calculations of this decoupling parameter are plotted against the persistence time in the inset of Fig. 9. We find that to within our numerical accuracy the data is well fit by $R \approx 3.95 + 1.0 \log(\tau_p / \tau_0)$. In earlier work using a simpler “cage escape”

model [21] we found $R \approx 3.2 + 1.5 \log(\tau_{cage} / \tau_0)$ or $R \approx (1.0 + 0.25 \log(\tau_{cage} / \tau_0))^2$. As previously discussed in that reference, the latter agrees well with hard sphere simulations, and also decoupling experiments on molecular liquids at T_g ; these forms are also quite similar to earlier estimates based on the single-particle NLE theory which fully took into account trajectory fluctuations (dynamic disorder) by numerically solving the stochastic equation-of-motion [37]. The quantitative similarity between the aforementioned studies again points to the degeneracy of theoretical approaches to the glass problem, and also supports our belief of strong connections between slow single-particle and many-particle activated dynamics.

VI. CONCLUSION AND OUTLOOK

We have extended our NLE theory of two-particle activated hopping in the glassy fluid regime [21] to treat multiple space-time correlated hopping, caging, and re-hopping events. This allowed the construction of simple models for the dynamics of neighbor loss and recovery that underlie the structural relaxation process. Comparisons with available simulations and colloid experiments reveal at least qualitative agreement. Our ability to define an “irreversible” event allows contact to be made with concepts that underlie kinetically constrained models. In particular, we found persistence times that are well-described by the KCM-inspired parabolic law [47], decoupling is reasonably well accounted for based on differences between mean persistence and exchange times, and some more general features of the persistence and exchange time distributions are in qualitative accord with simulations of KCMs and coarse-grainings of atomistic glass-formers [45]. A general point is that by combining our microscopic theory for space-time correlated hopping with an intuitive picture of following the dynamics of how two

particles separate through multiple correlated hopping and re-caging processes starting from some initial configuration, we have suggested concrete *structural-based* connections with diverse ways of thinking about the glass problem.

Our perspective in extending the single-particle NLE to the two-particle level is that cooperative rearrangements seem to involve many small motions combined with a few larger, particle-radius-scale attendant displacements, which in sum are related to unrecoverable thermal strains [41,50]. The hope is that in the context of a dynamic mean-field theory one can capture information about the whole rearrangement event with a coarse-grained description of these larger motions. It is in this sense we expect the present two-particle approach to be more representative of structural relaxation events in real glass-forming liquids than the earlier single-particle activated dynamics NLE approach. Better still would be a microscopic activated-event theory which includes a collective mode(s) involving a cluster of particles that undergo a diversity of correlated displacements— a daunting challenge for a force-based theory.

Quantitative comparisons of our theoretical results with experiments and simulations are presently limited for several reasons, including the fact the theory is for 3D fluids while the former have been largely focused on 2D systems. Future work could generalize the theory to two dimensions, and new 3D simulations could also be performed to more critically test our ideas. Additionally, while the focus here has been on hard spheres for simplicity, extension to other potentials for spherical particles is in principle straightforward, as has been extensively achieved in diverse contexts based on the single particle NLE approach [11]. In colloidal systems, the presence of short-range attractive forces and/or shape anisotropy can result in qualitatively new behaviors, and it could be interesting to study such systems from the perspective proposed here.

At present, the multi-state Markov framework has been developed only out to the third shell of the radial distribution function, but in principle it can be extended much further. In addition to suggesting a new approximation for the distinct van Hove function as outlined in the Appendix, this would allow new questions to be addressed. A natural next step might be to continue building up the Markov model to fully address the problem of 2-particle “unbinding.” That is, the process of two particles starting at contact and then separating to such a point that their motion becomes dynamically uncorrelated. The length and time scales over which that occurs are a key metric of dynamic heterogeneity.

Acknowledgments. We thank David Chandler and Peter Harrowell for valuable comments on this manuscript and correspondence. This work was supported by the Nanoscale Science and Engineering Initiative of the National Science Foundation under NSF Award DMR-0642573.

APPENDIX: New Approximation for the Distinct van Hove Function

Continuous time random walk (CTRW) models, in which a walker takes a step of random size at random points in continuous time [51], have been used in diverse phenomenological descriptions of amorphous materials [52, 53]. Persistence and exchange events have been embedded in this formalism as a way of translating distributions of events into an expression for the self-part of the van Hove function, $G_s(r, t)$, where two distinct time-scales are necessary to recover the correct expression for the van Hove function [54]. The essence of this approach is to take the distribution of displacements associated with persistence and exchange events to be $f_p(r)$ and $f_x(r)$, where $f_p(r)$ is associated with intra-cage local Gaussian vibrations, and the distribution of jump sizes associated with $f_x(r)$ might similarly be drawn from a Gaussian

distribution but with a larger characteristic length, e.g., $\sim \sigma/2$. Defining probability distributions for the times at which these events occur, $\phi_p(t)$ and $\phi_x(t)$, the probability that the random variable X of interest (for instance G_s) has the value r at time t is given by

$$X(r, t) = \sum_{n=0}^{\infty} p(n, t) f(n, r), \quad (21)$$

where $p(n, t)$ is the probability that the variable undergoes exactly n jumps in time t , and $f(n, r)$ is the probability that in n jumps the displacement is r . With the above distributions the CTRW framework allows one to carry out the sum in Fourier-Laplace space, with the result [54]

$$X(q, s) = f_p(q) \frac{1 - \phi_p(s)}{s} + f_p^2(q) f_x(q) \frac{\phi_p(s)(1 - \phi_x(s))}{s(1 - \phi_x(s) f_p(q) f_x(q))}. \quad (22)$$

This sort of formula can be (and has been [55, 56]) used to write down an expression for $G_s(r, t)$ or $F_s(k, t)$ given information from a single-particle theory about localization, jump distances, and average hopping and reaction times. In the KCM perspective of persistence and exchange events the expression is largely the same, except the distributions of persistence and exchange jumps are both taken to be drawn from the same (Gaussian) distribution [55].

Our theory of two-particle hopping is not suitable for studying the *self* part of the van Hove function because the jumps are not single particle events. However, if the analysis in section V is embedded in a CTRW framework one could construct a theory for a variable $X(r, t)$ that gives the probability that two particles with initial separation r_0 are separated by $r_0 + r$ at time t . In this Appendix, we sketch an idea for how information of this sort might be used to improve on the standard Vineyard approximation and estimate the *distinct* part of the van Hove function, $G_d(r, t)$.

First, one imagines coarse graining over the shells of the radial distribution and proceeds as outlined in section V, defining the *set* $X(r, t; i)$ for each shell i . Vineyard's original idea was to write the convolution [57]

$$G_d(r, t) = \int d\vec{r}' g(\vec{r}') H(\vec{r}, \vec{r}', t), \quad (23)$$

defining the unknown function G_d in terms of the unknown function H , and then making the approximation $H(\vec{r}, \vec{r}', t) \approx G_s(\vec{r} - \vec{r}', t)$. As a first step, motivated by the above discussion, one could alternatively approximate

$$H(\vec{r}, \vec{r}', t) \approx X(|\vec{r} - \vec{r}'|, t; i_{|\vec{r} - \vec{r}'|}). \quad (24)$$

where i is the shell of $g(r)$ indicated by the value of $|\vec{r} - \vec{r}'|$. Indeed, one could coarse grain to any desired degree – doing so exploits the observation that relative particle hops take (on average) particles from one shell to the next. This improves on the usual Vineyard approximation in two ways: first, the convoluting function for the radial distribution function is not identical to the single-particle time evolution, G_s , but rather is a genuine two-particle function, and second the convolution function itself varies with displacement. While the numerical work necessary to carry out this scheme is non-trivial, it may nevertheless prove useful to go beyond the venerable Vineyard approximation.

References

- [1] K. Ngai, *J. Non-Cryst. Solids* **275**, 7 (2000).
- [2] M. D. Ediger, *Annu. Rev. Phys. Chem.* **51**, 99 (2000).
- [3] J. Dyre, *Rev. Mod. Phys.* **78**, 953 (2006).
- [4] L. Berthier and G. Biroli, *Rev. Mod. Phys.* **83**, 587 (2011).
- [5] G. Tarjus in *Dynamical Heterogeneities in Glasses, Colloids, and Granular Media*, edited by Ludovic Berthier, Giulio Biroli, Jean-Philippe Bouchaud, Luca Cipelletti, Wim Van Saarloos (Oxford University Press, Oxford, 2011).
- [6] W. Götze and L. Sjögren, *Rep. Prog. Phys.* **55**, 241 (1992); W. Götze, *J. Phys.: Condens. Matter* **11**, A1 (1999); S. Das, *Rev. Mod. Phys.* **76**, 785 (2004).
- [7] W. Götze and L. Sjögren, *Z. Phys. B* **65**, 415 (1987).
- [8] W. Götze, “*Complex Dynamics of Glass-Forming Liquids: A Mode-Coupling Theory*” (Oxford University Press, 2009).
- [9] K. S. Schweizer, *Curr. Opin. Colloid Interface Sci.* **12**, 297 (2007).
- [10] K. S. Schweizer and E. J. Saltzman, *J. Chem. Phys.* **119**, 1181 (2003).
- [11] see, e.g. M. Tripathy and K. S. Schweizer, *Phys. Rev. E* **83**, 041406 (2011) and references therein
- [12] K. Chen, E. J. Saltzman, and K. S. Schweizer, *Annu. Rev. Condens. Matter Phys.* **1**, 277 (2010).
- [13] T. R. Kirkpatrick and P. G. Wolynes, *Phys. Rev. A* **35**, 3072 (1987).
- [14] H. Miyagawa, Y. Hiwatari, B. Berne, and J. P. Hansen, *J. Chem. Phys.* **88**, 3879 (1988).

- [15] R. Yamamoto and A. Onuki, Phys. Rev. E **58**, 3515 (1998); Phys. Rev. Lett. **81**, 4915 (1998).
- [16] W. van Megan, T. C. Mortensen, S. R. Williams, and J. Müller Phys. Rev. E **58**, 6073 (1998).
- [17] R. C. Kramb, R. Zhang, K. S. Schweizer, and C. F. Zukoski, Phys. Rev. Lett. **105**, 055702 (2010).
- [18] Y. L. Chen and K. S. Schweizer, J. Chem. Phys **120**, 7212 (2004).
- [19] L. Berthier and G. Tarjus, Phys. Rev. E **82**,031502 (2010).
- [20] L. Berthier and G. Tarjus, Eur. Phys. J. E **34**, 96 (2011).
- [21] D. M. Sussman and K. S. Schweizer, J. Chem. Phys. **134**, 064516 (2011)
- [22] S. K. Kumar, G. Szamel, and J. F. Douglas, J. Chem. Phys. **124**, 214501 (2006).
- [23] S. Swallen, K. Traynor, R. J. McMahon, and M. D. Ediger, J. Phys. Chem. B, **113**, 4600 (2009).
- [24] A. Widmer-Cooper, H. Perry, P. Harrowell, and D. R. Reichman, J. Chem. Phys. **131**, 194508 (2009).
- [25] K. Vollmayr-Lee, J. Chem. Phys. **121**, 4781 (2004).
- [26] A. Ghosh, V. Chikkadi, P. Schall, and D. Bonn, Phys. Rev. Lett. **107**, 188303 (2011).
- [27] J. P. Garrahan and D. Chandler, Proc. Natl. Acad. Sci. U.S.A. **100**, 9710 (2003).
- [28] D. Chandler and J. P. Garrahan, J. Chem. Phys. **123**, 044511 (2005).
- [29] A. S. Keys, L. O. Hedges, J. P. Garrahan, S. C. Glotzer, and D. Chandler Phys. Rev. X **1**, 021013 (2011).
- [30] E. Rabani, J. D. Gezelter, and B. J. Berne, Phys. Rev. Lett. **82**, 3649 (1999).
- [31] K. S. Schweizer, J. Chem. Phys. **123**, 244501 (2005).

- [32] J. P. Hansen and I. R. McDonald, *Theory Of Simple Liquids*, 3rd ed. (Academic Press, 2006).
- [33] K. S. Schweizer and G. Yatsenko, *J. Chem. Phys.* **127**, 164505 (2007).
- [34] K. S. Schweizer, *J. Chem. Phys.* **91**, 5802 (1989).
- [35] R. Zwanzig, *Nonequilibrium Statistical Mechanics* (Oxford University Press, 2001).
- [36] M. Guenza, *J. Chem. Phys.* **110**, 7574 (1999).
- [37] E. J. Saltzman, K. S. Schweizer, *Phys. Rev. E* **74**, 061501 (2006).
- [38] P. Hänggi, P. Talkner, and M. Borkovec, *Rev. Mod. Phys.* **2**, 251 (1990).
- [39] D. C. Viehman and K. S. Schweizer, *Phys. Rev. E* **78**, 051404 (2008).
- [40] E. R. Weeks, J. C. Crocker, A. C. Levitt, A. Schofield, and D. A. Weitz, *Science* **287**, 627 (2000).
- [41] P. Schall, D. A. Weitz, and F. Spaepen, *Science*, **318**, 1895 (2007).
- [42] G. A. Appignanesi, J. A. Rodriguez Fris, R. A. Montani, and W. Kob, *Phys. Rev. Lett.* **96**, 057801 (2006).
- [43] J. A. Rodriguez Fris, G. A. Appignanesi, and E. R. Weeks, *Phys. Rev. Lett.* **107**, 065704 (2011).
- [44] L. O. Hedges and J. P. Garrahan, *J. Phys. Condens. Matter* **19**, 205124 (2007).
- [45] L. O. Hedges, L. Maibaum, D. Chandler, and J. P. Garrahan, *J. Chem. Phys.* **127**, 211101 (2007).
- [46] D. Jeong, M. Y. Choi, H. J. Kim, and Y. J. Jung, *Phys. Chem. Chem. Phys.* **12**, 2001 (2010).
- [47] Y. S. Elmatad, D. Chandler, and J. P. Garrahan. *J. Phys. Chem. B.* **113**, 5563 (2009).
- [48] Y. J. Jung, J. P. Garrahan, and D. Chandler, *J. Chem. Phys.* **123**, 084509 (2005).
- [49] E. J. Saltzman and K. S. Schweizer, *J. Chem. Phys.* **125**, 044059 (2006).
- [50] A. Widmer-Cooper and P. Harrowell, *Phys. Rev. E* **80**, 061501 (2009).

- [51] E. W. Montroll and G. H. Weiss, *J. Math. Phys.* **6**, 167 (1965).
- [52] H. Scher and E. W. Montroll, *Phys. Rev. B* **12**, 2455 (1975).
- [53] C. Monthus and J.-P. Bouchaud, *J. Phys. A: Math. Gen.* **29**, 3847 (1995).
- [54] J. K. E. Tunaley, *Phys. Rev. Lett.* **33**, 1037 (1974).
- [55] L. Berthier, D. Chandler, and J. P. Garrahan, *Europhys. Lett.* **69**, 320 (2005).
- [56] E. J. Saltzman and K. S. Schweizer, *Phys. Rev. E* **77**, 051504 (2008).
- [57] G. H. Vineyard, *Phys. Rev.* **110**, 999 (1958).

FIGURE CAPTIONS

Figure 1. Representative dynamic free energy surface at $\phi = 0.55$ and $r_0 = 1.0$.

Figure 2. Relative-separation barrier heights in the (A) forward (r^+) and (B) backwards (r^-) directions versus initial separation for $\phi = 0.54 - 0.6$ (in increments of 0.01, bottom to top)

Figure 3. Relative-separation hopping times in the (A) forward (r^+) and (B) backwards (r^-) directions versus initial separation for $\phi = 0.54 - 0.6$ (in increments of 0.01, bottom to top), along with the interpolation curves (see text).

Figure 4. (A) Schematic cartoon of forward/backwards barriers at different initial separations. The differently-hatched regions correspond to coarse-grained sites. (B) Schematic cartoon of coarse-graining $g(r)$ into (left) a 4-state Markov model and (right) persistence/exchange events, defined as a near-neighbor pair of particles first separating and then moving farther away, respectively.

Figure 5. (A) Probability of neighbor loss/recovery at the cage-escape time, $P_{n,x}(\tau_{cage})$, for $x = 2, 3, 4, 6, 9$. Inset. Fraction of irreversible jumpers for $\tau = 0.5\tau_{cage}$ (dashed), τ_{cage} (solid), and $2\tau_{cage}$ (dash-dotted). (B) $P_{n,x}(\tau_{cage})$ for (left) $x = 3$ and (right) $x = 6$ at $\tau = 0.5\tau_{cage}$, τ_{cage} , $2\tau_{cage}$ (dashed, solid, and dash-dotted curves, respectively) at $\phi = 0.52$.

Figure 6. Probability distribution to first lose four neighbors, $P_4(t/\tau_{cage})$, for $\phi = 0.52$ (solid curve) and $\phi = 0.55$ (dashed curve). Inset. $P_4(t/\tau_{cage})$ at short times.

Figure 7. Logarithmic probability distributions for the exchange ($P(\log_{10} \tau_x)$, dashed) and persistence times ($P(\log_{10} \tau_p)$, solid) for $\phi = 0.52, 0.54, 0.56, 0.58, 0.6$.

Figure 8. $P(\log_{10} \tau_x)$ normalized by its peak height and position. Inset. $P(\log_{10} \tau_p)$ normalized by its peak height and position.

Figure 9. Average persistence time (circles), exchange time (diamonds), and cage escape time (triangles) as a function of volume fraction, and an empirical “parabolic law” fit to the persistence time, $\ln(\tau_p / \tau_0) \approx 480(\phi - 0.47)^2$. Inset. Decoupling parameter $R = \tau_p / \tau_x$. Solid line is $R = 3.9 + \log(\tau_p / \tau_0)$, and dashed lines are earlier decoupling predictions based on the “cage escape” model [21], $R = 3.2 + 1.5 \log(\tau_p / \tau_0)$ and $R = (2 + 0.25 \log(\tau_p / \tau_0))^2$.

FIGURES

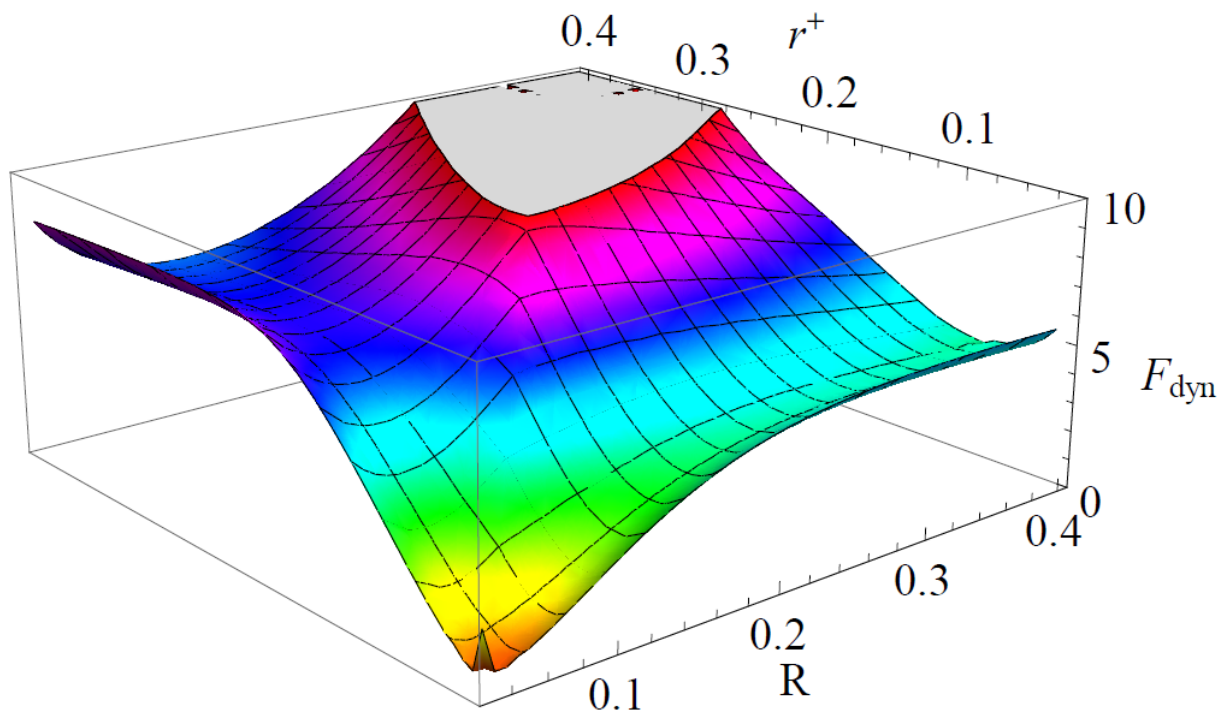


Figure 1.

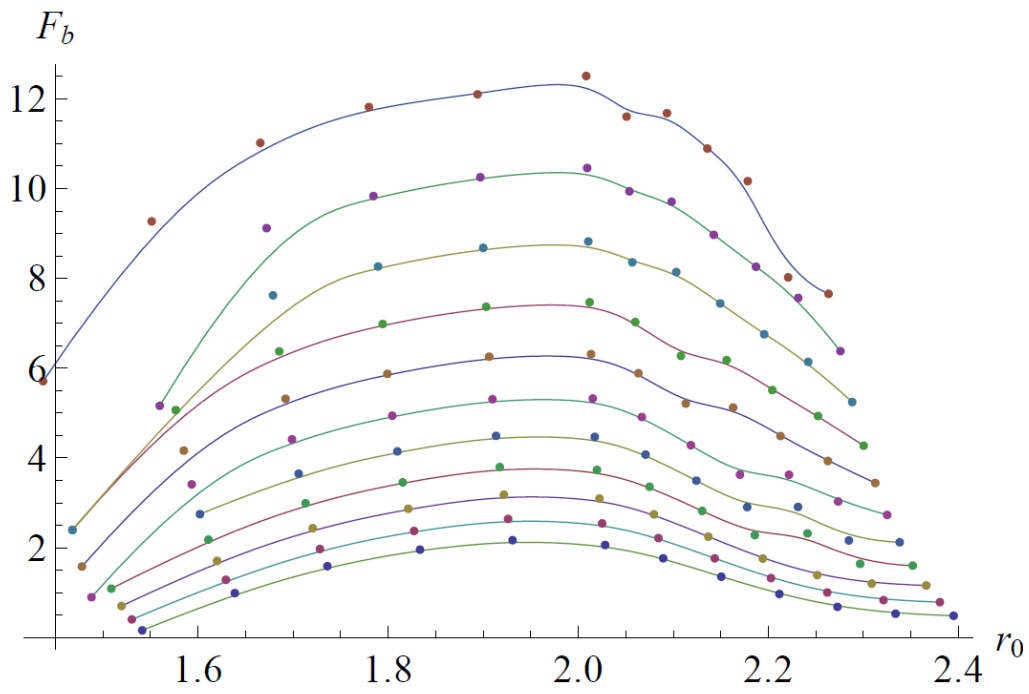
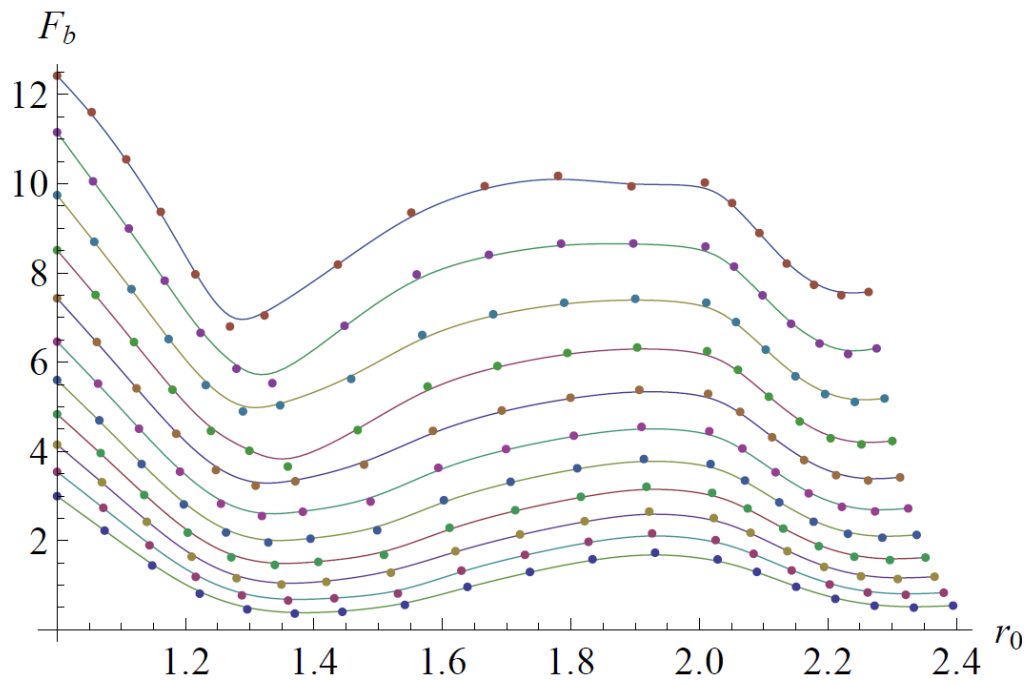


Figure 2 A and B

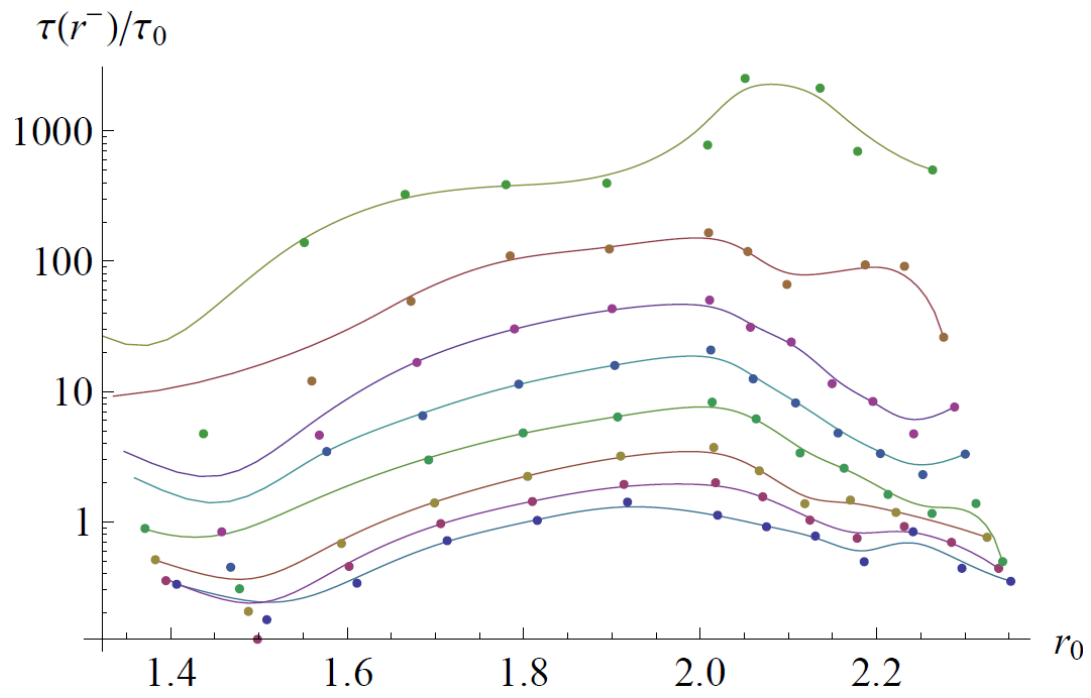
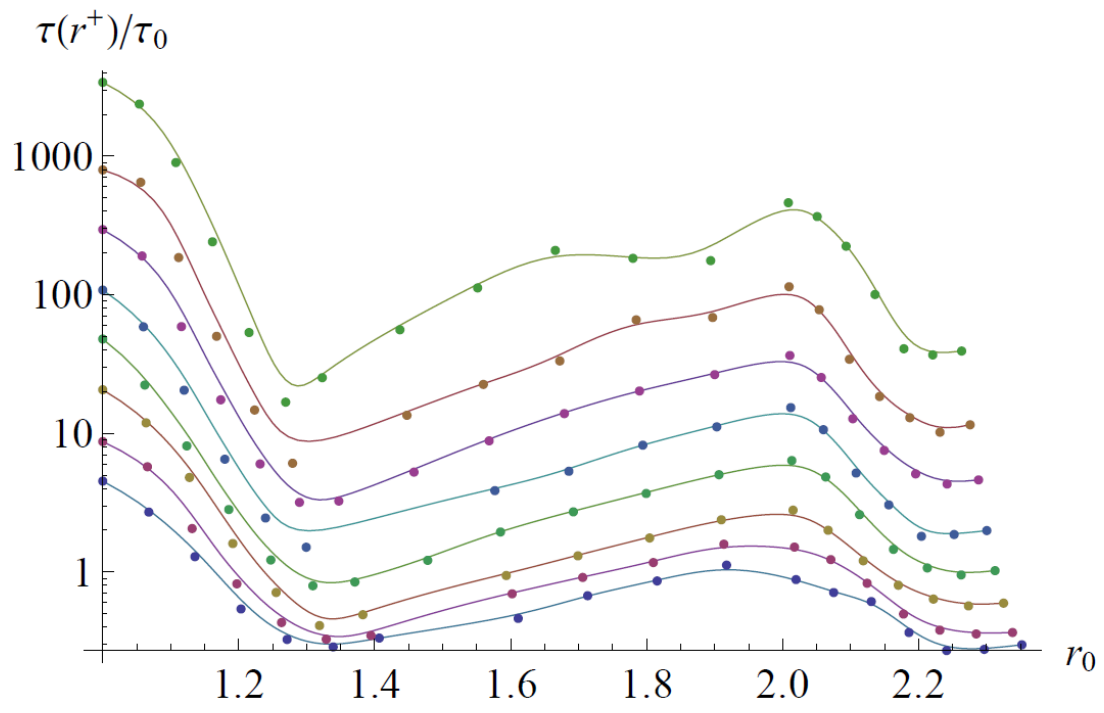


Figure 3 A and B

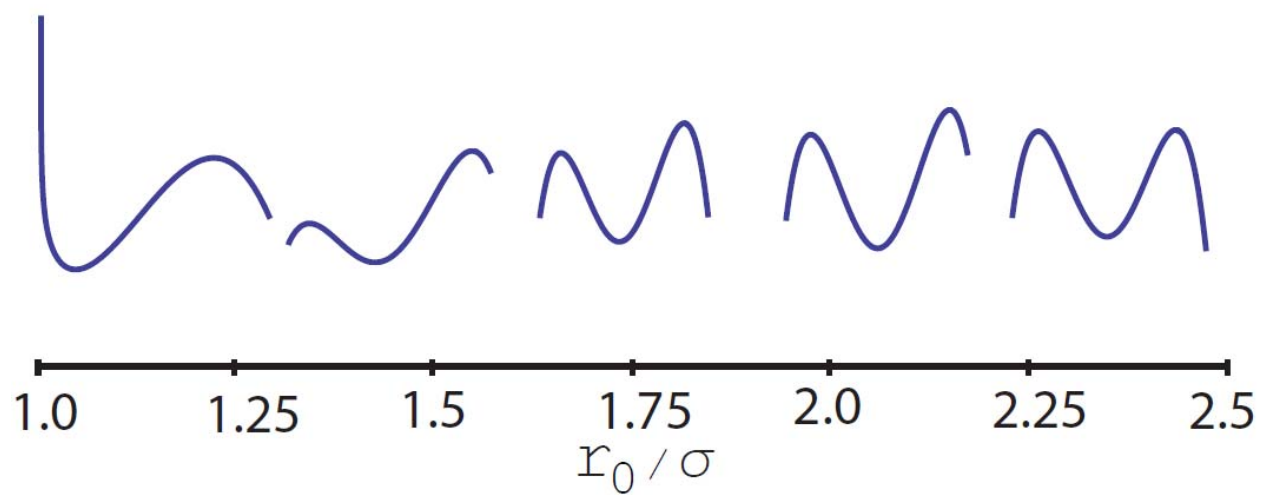


Figure 4A

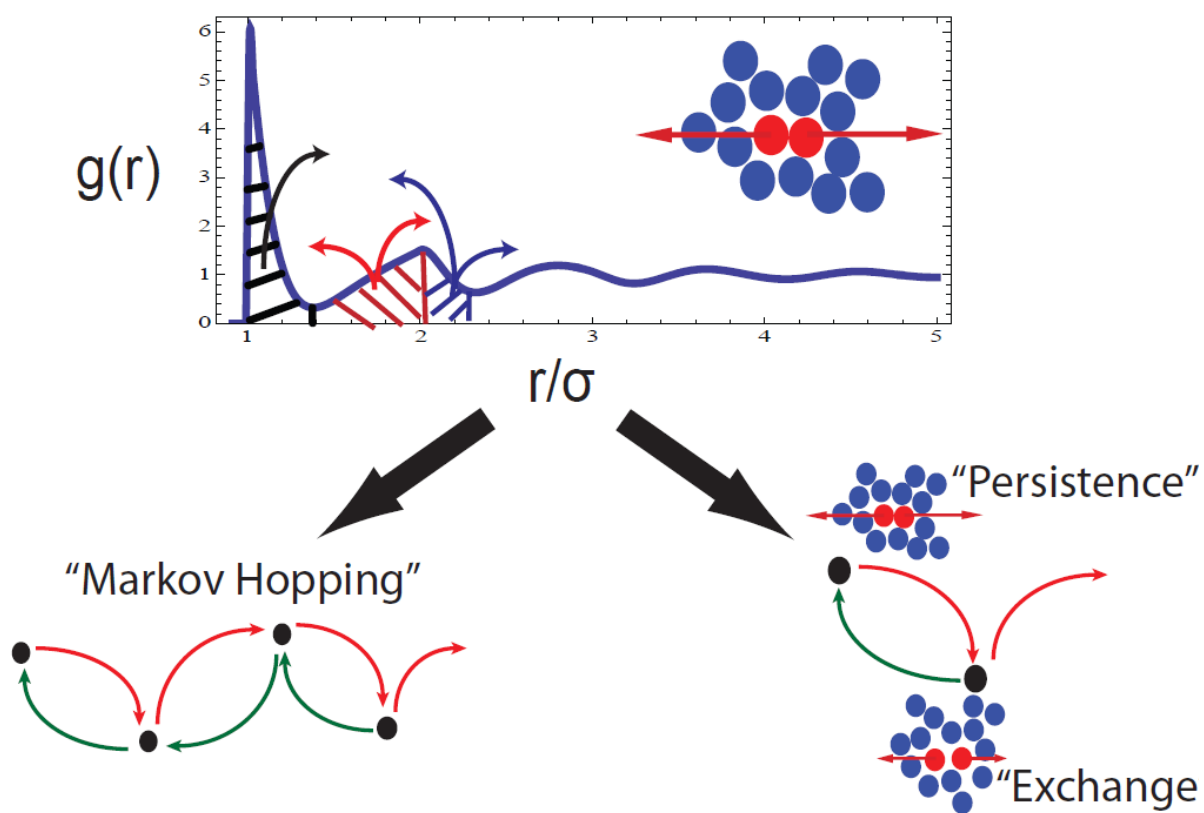


Figure 4B

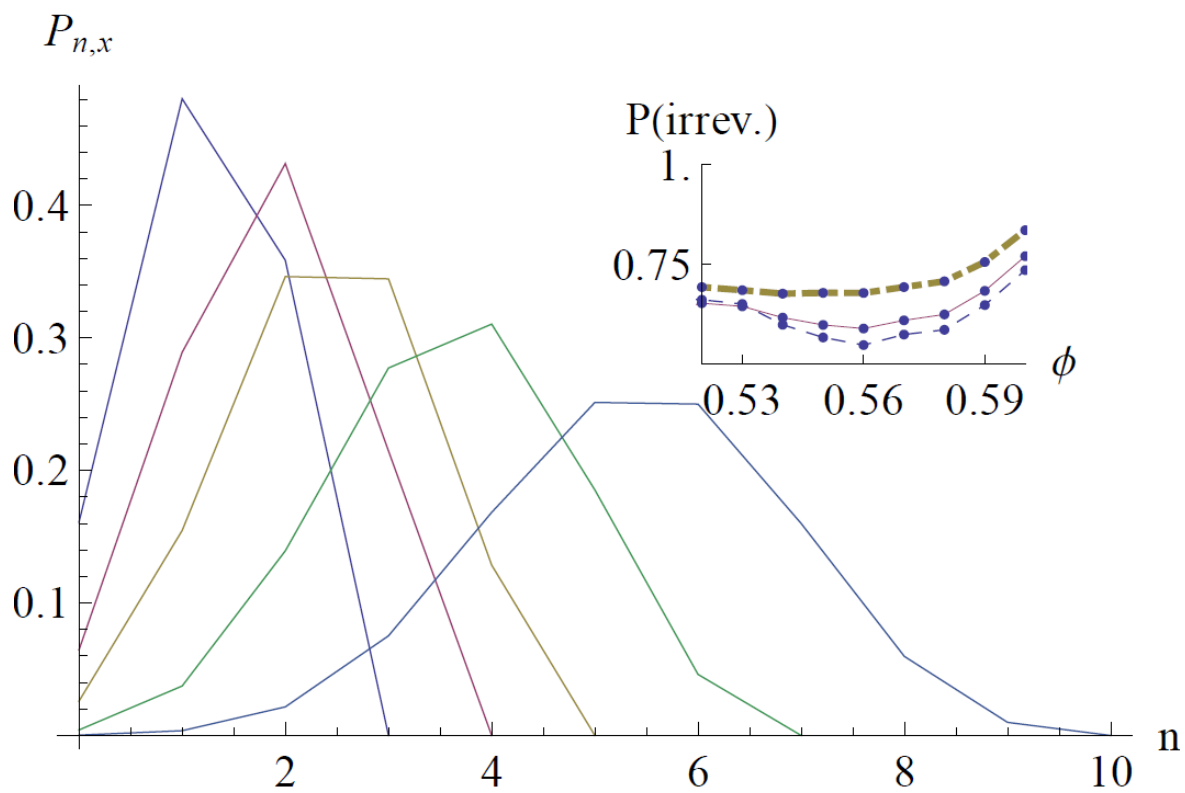


Figure 5 A

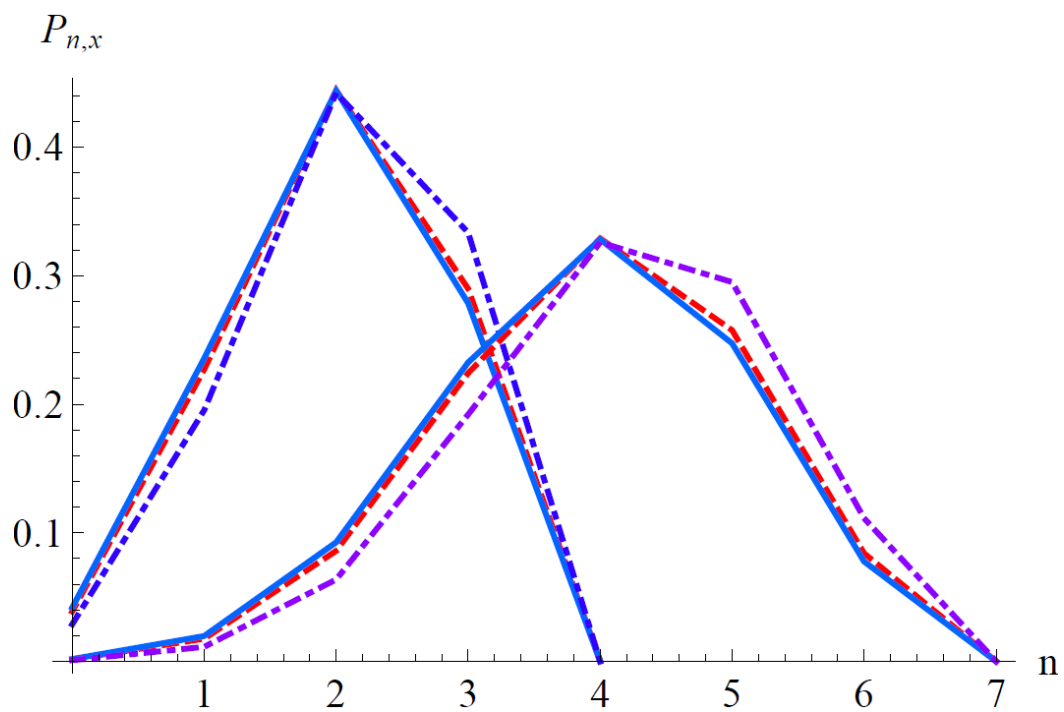


Figure 5B

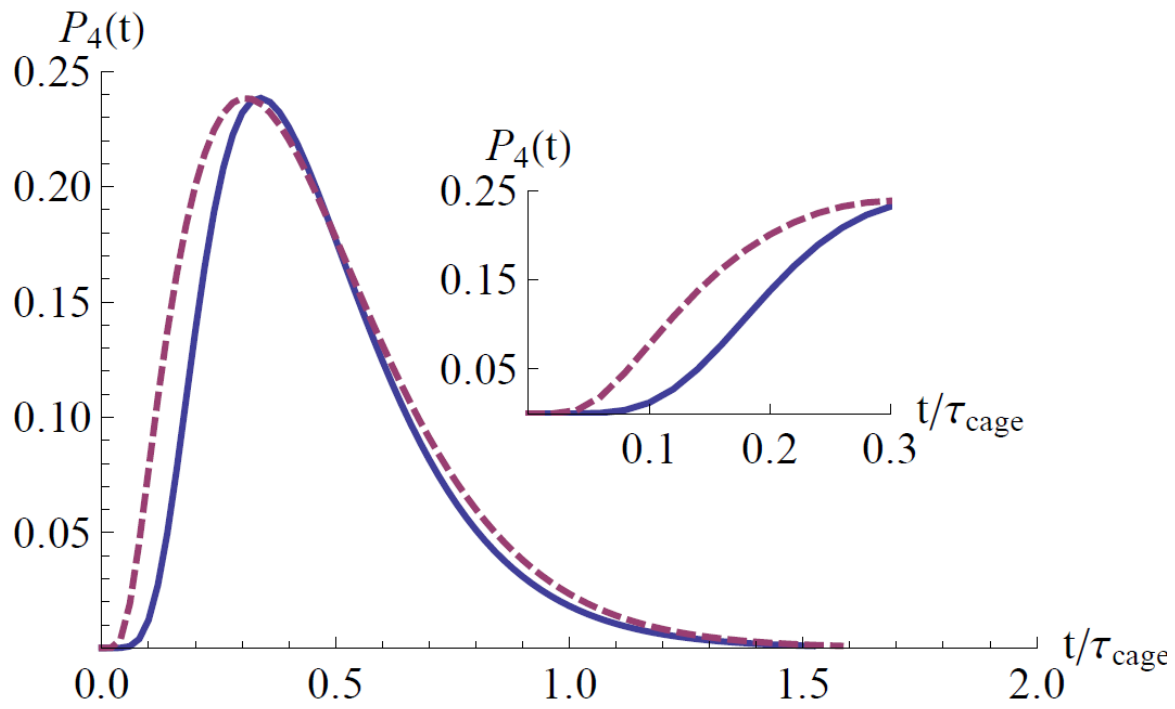


Figure 6.

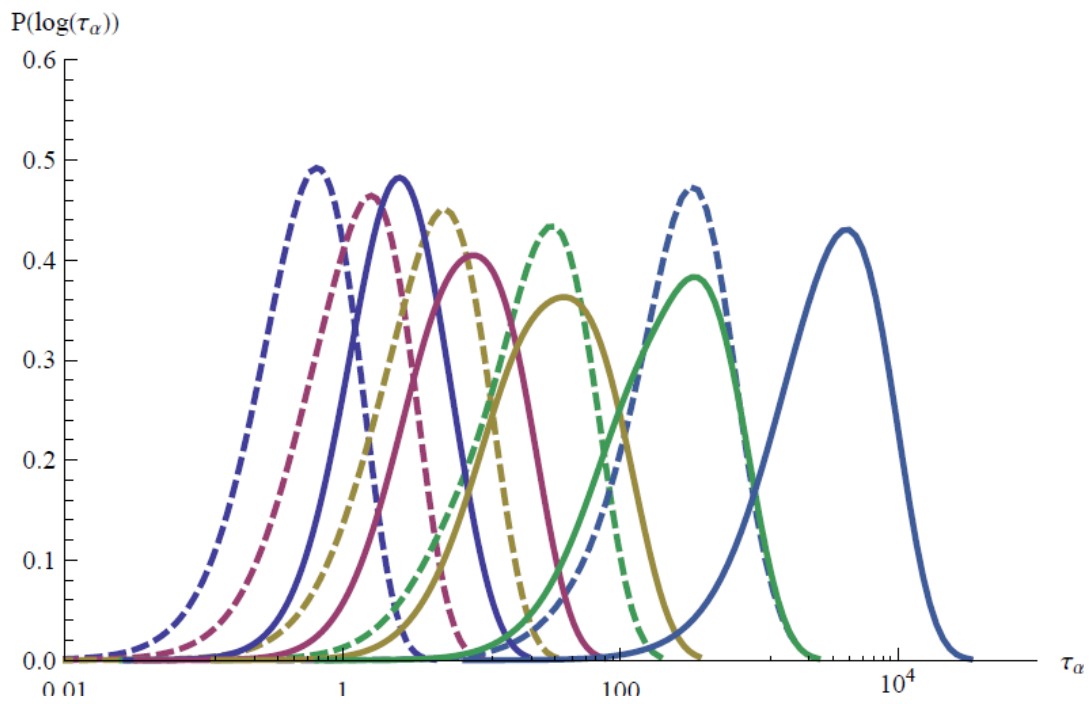


Figure 7

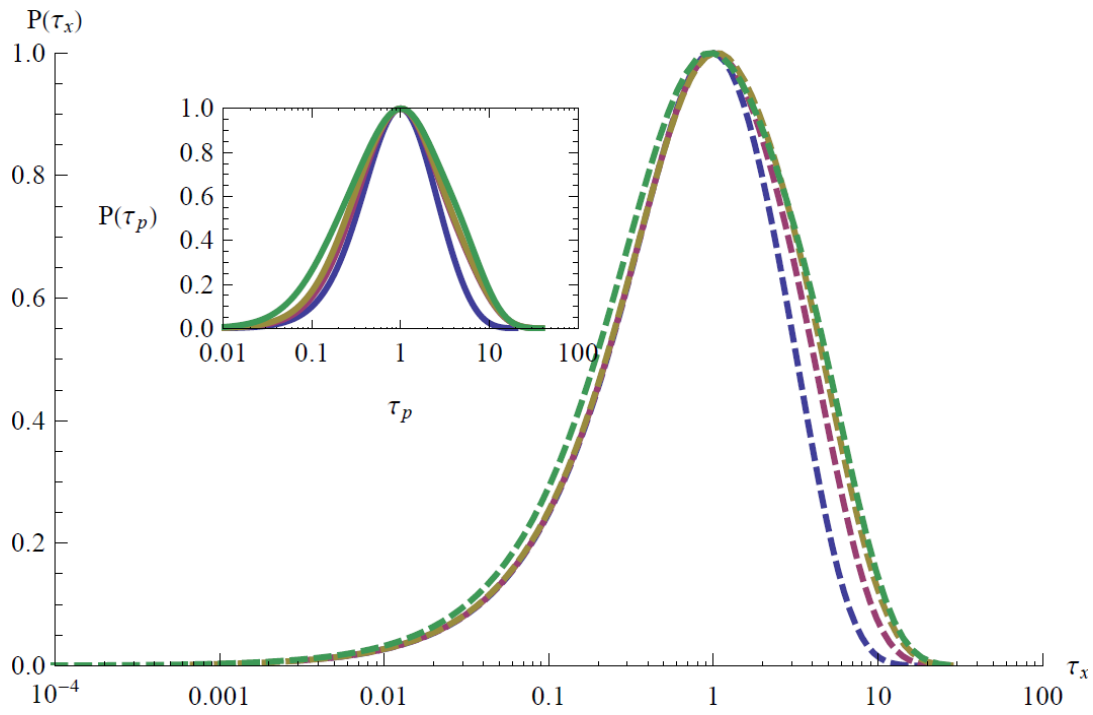


Figure 8

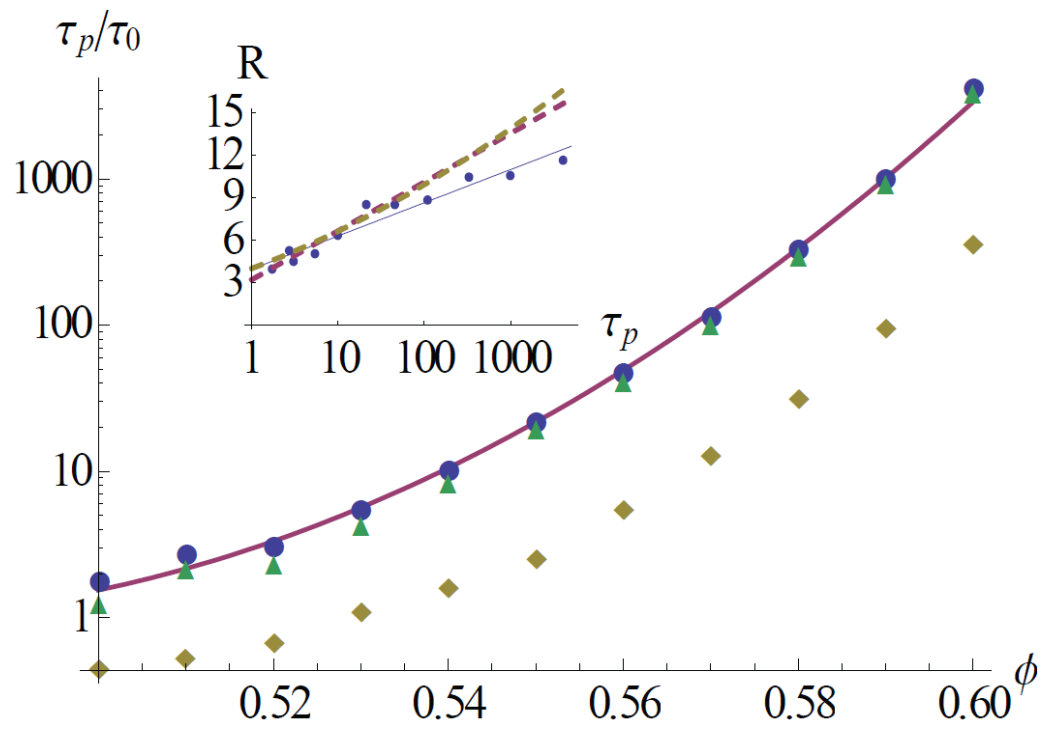


Figure 9